



On period doubling bifurcations of cycles and the harmonic balance method

Griselda R. Itovich^{a,*}, Jorge L. Moiola^b

^a *Departamento de Matemática, FAEA, Universidad Nacional del Comahue, Neuquén Q8300BCX, Argentina*

^b *Departamento de Ingeniería Eléctrica y de Computadoras Universidad Nacional del Sur, Bahía Blanca B8000CPB, Argentina*

Accepted 4 April 2005

Abstract

This work attempts to give quasi-analytical expressions for subharmonic solutions appearing in the vicinity of a Hopf bifurcation. Starting with well-known tools as the graphical Hopf method for recovering the periodic branch emerging from classical Hopf bifurcation, precise frequency and amplitude estimations of the limit cycle can be obtained. These results allow to attain approximations for period doubling orbits by means of harmonic balance techniques, whose accuracy is established by comparison of Floquet multipliers with continuation software packages. Setting up a few coefficients, the proposed methodology yields to approximate solutions that result from a second period doubling bifurcation of cycles and to extend the validity limits of the graphical Hopf method.

© 2005 Elsevier Ltd. All rights reserved.

1. Introduction

When a differential system satisfies the hypotheses of the Poincaré–Andronov–Hopf theorem, then a periodic solution or limit cycle appears after a smooth variation of a distinguished bifurcation parameter μ . Depending on the mathematical modeling and the pursued aims, one can use a numerical technique (simulation) to move along the emergent orbit or else one can try to find an approximate analytical expression. Different methods such as multiple scales, center manifold reduction and normal forms enable to fulfill the last possibility. Another alternative is the usual treatment of Hopf bifurcation in the frequency domain, called for simplicity graphical Hopf method, from which a quasi-analytical expression of the limit cycle can be obtained by means of harmonic balance techniques [1,17,18]. The accuracy provided by this methodology is based in the quantity of harmonics that are involved in the final expression of the cycle, and can be measured through the associated monodromy matrix, monitoring the error in the computation of the trivial multiplier +1 [24]. It must be taken into account that the suggested method has local validity, namely, close to Hopf bifurcation (also called as *primary* bifurcation), and whenever the established periodic solution has small amplitude. Varying one or more parameters of the original system, it is possible that the cycle undergoes a *secondary* bifurcation, changing its stability and giving place to, at least, one new periodic or quasi-periodic solution. Particularly, a solution whose period duplicates the one of the preexisting orbit is known as a new subharmonic solution and the phenomenon is called

* Corresponding author.

E-mail addresses: gitovich@arnet.com.ar (G.R. Itovich), jmoiola@criba.edu.ar (J.L. Moiola).

flip or period doubling bifurcation of cycles. Forced vibrations models described by Duffing type equations and well-known autonomous systems as Lorenz's, Rössler's and Chua's experiment qualitative changes in its solutions that include bifurcations of this kind. Frequently, the described situation repeats infinite times, generating the so-called period doubling cascade and the final stage is the appearance of a chaotic attractor. During 1970s, the studies of Feigenbaum attain to formalize this chaos route for maps, giving its universal characterization.

Within the works related with this topic but now in ODEs, Rand [21] sets up a starting point considering the problem of detecting a flip bifurcation and analyzing the stability change of the Hopf cycle through center manifold techniques. This phenomenon has captured the attention of Belhaq and Houssni [2] for the first period doubling, and later of Belhaq et al. [3] for the second period doubling. From the frequency domain point of view, Floquet multipliers are commonly used to analyze bifurcations of cycles as can be seen in [5,6,29]. In the first work, the monodromy matrix and approximations of higher order Hopf cycles are the keys to detect the appearance of a subharmonic solution. Related with feedback systems, a solid application of harmonic balance techniques to analyze period doubling bifurcation and approximate the resultant orbits, specially directed to bifurcation control, is developed in [27]. Flip bifurcations have particular interest due to its frequent relationship with chaotic behavior: this can be seen in the analysis of certain electric power systems [4,26], in the frontier of the harmonic distortion of electronic oscillators [15] or in some kind of switched reluctance motors [7]. On the other hand, this type of bifurcation is recurrent when complex biological systems are studied, i.e., in medicine, such as the brain activity in an epilepsy model [20] or cardiac work previous to a severe arrhythmia [25].

In this manuscript, quasi-analytical expressions which involve up to eight harmonics are used to approximate periodic solutions that result from a dynamic or Hopf bifurcation. Analyzing the closeness of the trivial Floquet multiplier to the value +1, the limit of the local approximation of the branch of cycles (starting from Hopf bifurcation) will be derived. At the same time, an alternative proposal to obtain an approximation of the cycle, which also uses harmonic balance, is presented. It intends to extend the established limits through the classic frequency treatment. Otherwise, if varying the bifurcation parameter μ , one characteristic multiplier of a generic cycle crosses the unit circle through -1 , then a flip or period doubling bifurcation appears. When this phenomenon takes place close to the Hopf bifurcation value, it may be determined how the bifurcation of cycles occurs, namely, where the subharmonic solution appears, how is its quasi-analytical expression and which are its dynamical properties. The starting point will be the known information about the amplitude and frequency of the Hopf cycle, which changes its stability at flip bifurcation. The results will be compared with those obtained with LOCBIF [12], through Floquet multipliers. The continuation of this new branch of periodic solutions will allow to estimate the second period doubling bifurcation and, by making an adjustment of the proposed method, the orbits coming from the last bifurcation may also be approximated. A closely related technique has been proposed recently in Chung et al. [8] for detecting accurately the period doubling bifurcation but not necessarily in the vicinity of a Hopf bifurcation.

This work is organized as follows: the foundation of the treatment of Hopf bifurcation in the frequency domain is set in Section 2 and a summary of results about stability and bifurcations of cycles can be found in Section 3. Afterwards, the subharmonic solutions which appear from a supercritical period doubling bifurcation are analyzed in Section 4 and a simple methodology to obtain an approximation of them is proposed. Two examples are fully developed in Section 5 and at last, the conclusions are reported in Section 6.

2. Basic concepts

It is considered an n -dimensional nonlinear differential system like

$$\dot{x} = f(x; \mu), \quad (1)$$

where $\dot{x} = \frac{dx}{dt}$, $x \in R^n$, $f \in C^r$, $r \geq 9$ and $\mu \in R$. It is supposed that \bar{x} is an equilibrium point ($f(\bar{x}; \mu) = 0$) and μ is a distinguished bifurcation parameter of system (1). This problem can be expressed equivalently including new input and output variables, say $u \in R^p$ and $y \in R^m$, and formulated as a feedback system. Thus, one obtains the following mixed representation with a state variable x , an output variable y , and a nonlinear control u

$$\begin{aligned} \dot{x} &= A(\mu)x + B(\mu)D(\mu)y + B(\mu)u, \\ y &= C(\mu)x, \\ u &= g(e; \mu) = \tilde{g}(y; \mu) - D(\mu)y, \end{aligned} \quad (2)$$

where A is a $n \times n$ matrix (chosen for convenience, as invertible for every value of μ), B , C and D are matrices with orders $n \times p$, $m \times n$ and $p \times m$, respectively, \tilde{g} is a nonlinear function defined on R^p which results from the original

function f and the selection made for the matrices A , B , C and D , and $g \in C^r$, $r \geq 9$, where $e = -y$. This procedure constitutes what is known as a realization of system (1). Then, if one applies Laplace transform to system (2) with the initial condition $x(0) = 0$, the analysis of the feedback system proceeds by finding the equilibrium \tilde{e} , which is the solution of the equation

$$e = -G(0; \mu)g(e; \mu), \tag{3}$$

where $G(s; \mu) = C(\mu)[sI - (A(\mu) + B(\mu)D(\mu)C(\mu))]^{-1}B(\mu)$ is the usual transfer matrix of the linear part of system (2), being s the Laplace transform variable, and a nonlinear part represented by u , defined by $u = g(e; \mu)$ which can be thought as an input of the system. Carrying out a linearization of (2) and evaluating at the equilibrium \tilde{e} , one obtains a system whose Jacobian J is a $p \times m$ matrix given by

$$J = J(\mu) = D_1g(e; \mu)|_{e=\tilde{e}} = \begin{bmatrix} \frac{\partial g_j}{\partial e_k} \Big|_{e=\tilde{e}} \end{bmatrix}, \tag{4}$$

where $g = [g_1 \ g_2 \ \dots \ g_p]^T$, $j = 1, 2, \dots, p$, $k = 1, 2, \dots, m$. Then, the application of the generalized Nyquist stability criterion [14] provides the necessary conditions for the critical cases:

Lemma 1. *If the linearization of system (1) evaluated at \tilde{x} has an eigenvalue $i\omega_0$ when $\mu = \mu_0$ then the associated eigenvalue of the matrix $G(i\omega_0; \mu_0)J(\mu_0)$ evaluated at \tilde{e} takes the value $-1 + i0$ for $\mu = \mu_0$.*

The situation of Lemma 1 is related with the appearance of bifurcations in the solutions of system (1). If $\omega_0 \neq 0$ and some additional conditions are satisfied it is possible that a dynamic or Hopf bifurcation happens, which is linked with the creation or disappearance of periodic solutions.

Due to Lemma 1, it is known that if a bifurcation exists in (1) then

$$h(-1, i\omega; \mu) = \det(-1 \times I - G(i\omega; \mu)J(\mu)) = 0, \tag{5}$$

for a certain pair (ω_0, μ_0) . Eq. (5) can be transformed into an equivalent system of equations, splitting its real (Re) and imaginary (Im) parts, resulting

$$\begin{cases} F_1(\omega, \mu) = \text{Re}(h(-1, i\omega; \mu)) = 0, \\ F_2(\omega, \mu) = \text{Im}(h(-1, i\omega; \mu)) = 0. \end{cases}$$

Making use of the functions F_1 and F_2 , the next result can be formulated [18]:

Proposition 1. *If a dynamic or Hopf bifurcation exists at (ω_0, μ_0) , $\omega_0 \neq 0$, then follows:*

$$F_1(\omega_0, \mu_0) = F_2(\omega_0, \mu_0) = 0.$$

The Poincaré-Andronov-Hopf theorem [9] gives sufficient conditions to assure the appearance of a branch of periodic solutions in a system like (1). Its formulation in the frequency domain [17,18] is established through three fundamental hypotheses, in this way.

Theorem 1

(H1) *There is a unique complex function $\hat{\lambda}$, which solves $h(\hat{\lambda}, i\omega; \mu) = 0$, passes through $(-1 + i0)$ when ω goes through $(0, \infty)$ and involves a stability change of the equilibrium. Moreover, there is only one frequency $\omega_0 \neq 0$ which satisfies $h(-1, i\omega_0; \mu) = 0$ for a certain value $\mu = \mu_0$, and besides $\frac{\partial F_1}{\partial \omega} \Big|_{(\omega_0, \mu_0)}$, $\frac{\partial F_2}{\partial \omega} \Big|_{(\omega_0, \mu_0)}$ do not vanish simultaneously, avoiding any resonance case.*

(H2) *The determinant M_1 is nonzero, say*

$$M_1 = \begin{vmatrix} \frac{\partial(F_1, F_2)}{\partial(\omega, \mu)} \Big|_{\omega_0, \mu_0} \end{vmatrix} = \begin{vmatrix} \frac{\partial F_1}{\partial \omega} & \frac{\partial F_1}{\partial \mu} \\ \frac{\partial F_2}{\partial \omega} & \frac{\partial F_2}{\partial \mu} \end{vmatrix} \Big|_{(\omega_0, \mu_0)} \neq 0,$$

which is an equivalent expression for the nondegeneracy of the transversality condition of the classic formulation in time domain.

(H3) *The expression σ_1 , known as curvature coefficient and defined as follows:*

$$\sigma_1 = -\text{Re} \left(\frac{u^T G(i\omega_0; \mu_0) p_1(\omega_0, \mu_0)}{u^T G'(i\omega_0; \mu_0) J(\mu_0) v} \right), \tag{6}$$

has a sign definition. This coefficient can be calculated by other techniques and is also recognized as the first Lyapunov coefficient [13], cubic term coefficient in the normal form expansion [9], and so on.

Observation: In the last formula, u^T and v are the left and right normalized eigenvectors of the matrix $G(i\omega_0; \mu_0)J(\mu_0)$ associated with the eigenvalue $\hat{\lambda}$ ($\bar{u}^T v = 1$ and $\bar{v}^T u = 1$, where “ $\bar{\cdot}$ ” means complex conjugate), $G' = \frac{dG}{ds}$ and p_1 is a complex vector

$$p_1(\omega, \mu) = QV_{02} + \frac{1}{2}\bar{Q}V_{22} + \frac{1}{8}L\bar{v},$$

whose computation is based on the second and third derivatives of the function g [17], and Q, \bar{Q} and L are $p \times m$ matrices defined as

$$Q = Q(\mu) = D_2g(e; \mu)|_{e=\bar{e}}v = \left[\sum_{l=1}^m \frac{\partial^2 g_j}{\partial e_l \partial e_k} \Big|_{\bar{e}} v_l \right],$$

where $v = [v_1 \ v_2 \ \dots \ v_m]^T$, and

$$L = L(\mu) = D_3g(e; \mu)|_{e=\bar{e}}v \otimes v = \left[\sum_{l=1}^m \sum_{i=1}^m \frac{\partial^3 g_j}{\partial e_l \partial e_i \partial e_k} \Big|_{\bar{e}} v_l v_i \right],$$

where $j = 1, 2, \dots, p, k = 1, 2, \dots, m$. Furthermore, the following vectors are defined:

$$V_{02} = -\frac{1}{4}H(0; \mu)Q\bar{v}, \quad V_{22} = -\frac{1}{4}H(i2\omega; \mu)Qv,$$

where $H(s; \mu) = [I + G(s; \mu)J(\mu)]^{-1}G(s; \mu)$ is the so-called closed loop transference matrix.

Then a branch of periodic solutions starts at $\mu = \mu_0$, whose direction and stability result from the values of M_1 and σ_1 , respectively. When $\sigma_1 > 0$ follows that the solution will be unstable (subcritical Hopf bifurcation) or else stable if $\sigma_1 < 0$ (supercritical case).

The demonstration of the Poincaré-Andronov-Hopf theorem by using harmonic balance is constructive, namely, it allows to write an approximate expression of the periodic solution, after estimating its frequency ω and the amplitude θ of its first harmonics. These values can be interpreted as a part of a certain graphic in the complex plane and this is the reason for calling this formulation as the graphical Hopf theorem. More specifically, according with the behavior of the eigenlocus described by the critical eigenvalue $\hat{\lambda} = \hat{\lambda}(i\omega; \mu)$, one chooses $\tilde{\mu}$ next to μ_0 and searches for a first estimate of the frequency $\hat{\omega}$ through the intersection point between the eigenlocus and the real axis, which results nearest to $(-1 + i0)$. With this solution pair $(\hat{\omega}, \tilde{\mu})$, one computes the corresponding eigenvectors u^T, v , the complex vector p_1 and at last $\xi_1 = -u^T G(i\hat{\omega}; \tilde{\mu})p_1$. Then, it is considered a certain curve described by $L_1 = -1 + \xi_1 \theta^2$, as θ varies, which is called *amplitude locus*. The next step consists in looking for the intersection between the two mentioned loci. So, one obtains a new solution pair $(\hat{\omega}, \hat{\theta})$, where $\hat{\omega} = \hat{\omega}(\hat{\mu})$ and $\hat{\theta} = \hat{\theta}(\hat{\mu})$ are approximations for the frequency and the amplitude of the analyzed oscillation. Using second order harmonic balance, one calculates a semi-analytical approximate expression of the variable e which appears in the system (2) writing

$$e = e(t; \hat{\mu}) = \bar{e}(\hat{\mu}) + \text{Re} \left(\sum_{k=0}^2 E_k \exp(ik\hat{\omega}t) \right), \tag{7}$$

where $E_0 = \hat{\theta}^2 V_{02}, E_1 = \hat{\theta}v + \hat{\theta}^3 V_{13} = \hat{\theta}V_{11} + \hat{\theta}^3 V_{13}, E_2 = \hat{\theta}^2 V_{22}$. The vector V_{13} can be found taking in mind that

$$P[I + G(i\hat{\omega}; \hat{\mu})J(\hat{\mu})]V_{13} = -PG(i\hat{\omega}; \hat{\mu})p_1, \tag{8}$$

where $P = I - V_{11}V_{11}^T$, under the condition $V_{13} \perp V_{11}$. All the previous expressions which involve the nonlinear function g must be evaluated at the equilibrium $\bar{e} = \bar{e}(\hat{\mu})$.

The generalization of the described method with explicit fourth-order harmonic balance formulae appears in [16] and justifies the hypotheses established for the function $f(\cdot)$ and afterwards for $g(\cdot)$ at the beginning of this section. This extension allows to improve the approximations substantially, due to the use of better estimations of the frequency and amplitude of the oscillation. The details and explicit formulae for the computation involving up to eight harmonics can be found in [18]. One must keep in mind that these results are valid locally, in other words, when the parameter is close to the Hopf bifurcation value and besides when the analyzed cycles have small amplitude.

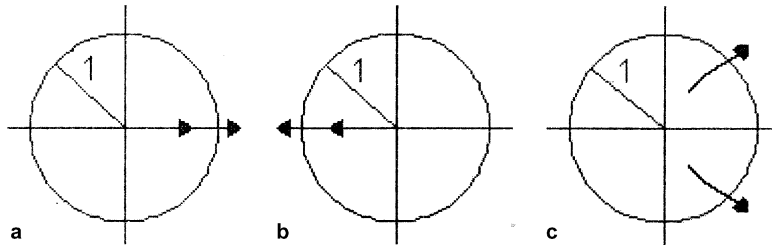


Fig. 1. Bifurcations of cycles: (a) fold, transcritical or pitchfork, (b) flip or period doubling, and (c) Neimark–Sacker.

3. Stability and bifurcations of cycles

If one has to analyze the stability of a periodic solution $\mathbf{X} = \mathbf{X}(t; \tilde{\mu})$ of a system as (1) two different tools can be applied at first, namely, Floquet theory and the dynamic analysis of discrete maps, the last one through the conception of the Poincaré or return map. Considering the first one which comes from the stability analysis on nonautonomous systems, the stability of the orbit \mathbf{X} is based on the study of the eigenvalues of the so-called monodromy matrix. This array is obtained from the general solution of the following differential equation

$$\dot{z} = D(t)z, \tag{9}$$

where $z \in R^n$, $\dot{z} = \frac{dz}{dt}$ and $D(t) = D_1 f(\mathbf{X}(t; \tilde{\mu}); \tilde{\mu}) = \frac{\partial f}{\partial x} |_{x=\mathbf{X}(t; \tilde{\mu}), \mu=\tilde{\mu}}$, $D(t + T) = D(t)$, being T the period of the cycle \mathbf{X} .

If one considers $M = M(t)$, a fundamental matrix of solutions of (9) such as $M(0) = I$, where I is the identity of order n , and computes $M(T)$, then the monodromy matrix of the orbit \mathbf{X} is obtained. The eigenvalues of this matrix are called Floquet or characteristic multipliers. It can be proved that one of the multipliers of a periodic solution of an autonomous system like (1) is always identically +1 [19] and this is the reason for evaluating the accuracy of a cycle approximation measuring the error in the computation of the trivial characteristic multiplier [24].

If two or more Floquet multipliers are placed on the unit circle, the periodic solution is called nonhyperbolic. Generally, this situation gives rise to a bifurcation of cycles, when the parameter μ varies. If one starts with a periodic solution that changes its stability at a certain value μ_1 , the resultant dynamics depends on the mode that the Floquet multipliers cross the unit circle (see Fig. 1). There are three possible cases: first, it can occur that one multiplier crosses the unit circle through the positive real axis (crosses by +1). In this case, the result is a fold (saddle-node), transcritical or pitchfork (symmetry-breaking) bifurcation of cycles, which involves at least two periodic solutions. Another situation is presented when one Floquet multiplier crosses the unit circle along the negative real axis (crosses by -1), and gives place to a flip or period doubling bifurcation of cycles, which implicates the appearance of a new periodic solution that rests over a Möbius band in R^n [28] and whose period doubles the period of the orbit \mathbf{X} . At last, if two complex conjugate Floquet multipliers cross the unit circle a secondary Hopf or Neimark–Sacker bifurcation occurs. This case is related with the appearance of a quasi-periodic solution which lives on a torus surface in R^n .

The two initial approaches considered for the stability analysis of the solution \mathbf{X} are connected finally through the following result [13]:

Theorem 2. *The eigenvalues of the monodromy matrix $M(T)$ are $\alpha_0 = 1$ and $\{\alpha_i\}_{i=1}^{n-1}$, where $\{\alpha_i\}_{i=1}^{n-1}$, are the eigenvalues of the linearization of the Poincaré or return map associated with the cycle \mathbf{X} .*

Observation: All the bifurcations of cycles mentioned above are recognized as local bifurcations, and one can find their equivalent bifurcations of fixed points in discrete systems through the abstraction of the Poincaré map.

4. Subharmonic or period doubling solutions

Suppose that a system like (1) has a periodic solution $\mathbf{X} = \mathbf{X}(t; \tilde{\mu})$ of frequency $\tilde{\omega}(\tilde{\mu})$ and for a certain value of the bifurcation parameter $\mu = \mu_1 \triangleq \mu_{PD2}$ a flip or period doubling bifurcation happens. Then a new subharmonic solution \mathbf{X}_{PD2} appears and its fundamental frequency is $\omega_{PD2} \approx \frac{\tilde{\omega}(\tilde{\mu})}{2}$. This observation is clearly reflected through the spectrum analysis [11,19] of the periodic solutions that coexist. Otherwise, thinking about the Poincaré map associated with the

solution \mathbf{X}_{PD2} , it can be inferred the existence of a cycle of period two and its stability agrees with the corresponding of \mathbf{X}_{PD2} .

The aforementioned bifurcation of cycles is of codimension 1, say, it is characterized through the changes of a unique parameter. Thus, supercritical and subcritical flip bifurcations can be distinguished, as in the Hopf bifurcation setting. In the supercritical case, one stable period-1 solution exists when $\mu < \mu_{\text{PD2}}$ while it becomes unstable for $\mu > \mu_{\text{PD2}}$ and, at the same time, a stable orbit of period-2 appears. This is the dynamic case that can be developed systematically in the following. Otherwise, the subcritical case corresponds to the appearance of an unstable period-2 orbit for $\mu < \mu_{\text{PD2}}$ coexisting with the stable period-1 oscillation.

The method described below is related with the basic idea of obtaining a quasi-analytical approximation for the new periodic solution which appears from flip bifurcation, about the determination of when it occurs exactly as well as its stability analysis. To specify the executed procedure, it is considered a system like (1), which has a supercritical Hopf bifurcation when $\mu = \mu_0 \triangleq \mu_{\text{H}}$. It is known that very accurate expressions can be obtained to recover the periodic solution \mathbf{X} which appears with $\tilde{\mu} > \mu_{\text{H}}$ ($\tilde{\mu}$ next to μ_{H}) thanks to the graphical Hopf method and its generalizations of higher order. Those results yield approximate values for the frequency of the cycle $\hat{\omega}(\tilde{\mu})$, whose exactness increases according with the number of harmonics that takes part in the approximations. Analyzing the progression of the characteristic multipliers of a generic cycle, it is observed that one of them crosses the unit circle through the real negative axis (by -1) when $\mu = \mu_{\text{PD2}}$ (it is supposed that μ_{PD2} is close to μ_{H}), giving place to a supercritical period doubling bifurcation. As the frequency $\hat{\omega}(\tilde{\mu})$ and the amplitude $\hat{\theta}(\tilde{\mu})$ of a Hopf cycle can be found with great accuracy, for any $\tilde{\mu}$ next and larger than μ_{PD2} then these values can be considered as the starting points to obtain the approximation of the period doubling orbit. Henceforth, let us call $\hat{\omega}$ the value of the frequency estimated by harmonic balance through the graphical Hopf method. Thus, it is proposed the following formula

$$\mathbf{X}_{\text{PD2}}(t; \tilde{\mu}) = (x_{i(\text{PD2})}(t; \tilde{\mu})) = \sum_{j=0}^4 a_{i,j}(\tilde{\mu}) \cos\left(j \frac{\hat{\omega}}{2} t\right) + \sum_{k=1}^4 b_{i,k}(\tilde{\mu}) \sin\left(k \frac{\hat{\omega}}{2} t\right), \quad (10)$$

that points out a Fourier partial sum, where $a_{i,j}$ and $b_{i,k}$, $i = 1, \dots, n$, are certain numerical vectors of R^n to determine, admitting that $\mathbf{X}_{\text{PD2}}(t; \tilde{\mu}) \rightarrow \mathbf{X}$, when $\tilde{\mu} \rightarrow \mu_{\text{PD2}}^+$, $a_{i,j}(\tilde{\mu}), b_{i,k}(\tilde{\mu}) \rightarrow 0$ for $j = k = 1, 3$, and the remaining coefficients of \mathbf{X}_{PD2} agree with those of the cycle \mathbf{X} in the limit.

Considering that it is attempted to establish a solution of the system (1), substituting (10) and applying harmonic balance of order four in the fundamental frequency $\frac{\hat{\omega}}{2}$, it is attained a nonlinear algebraic system. The corresponding computation is always performed through classical and commercial optimization routines and the results allow to determine the quasi-analytical expression for the period doubling orbit. Then, the existence of nontrivial solutions for the last system guarantees the character of the detected bifurcation of cycles. Moreover, the stability analysis of the bifurcated solution can also be stated through the monodromy matrix. It can be asserted that the proposed expression becomes more precise if the limit cycle that bifurcates has small amplitude and furthermore, if this phenomenon takes places when $\tilde{\mu}$ is close to the Hopf bifurcation value (as a consequence of the local validity of the classical Poincaré-Andronov-Hopf theorem). It can be observed that, $9n$ coefficients must be determined in the expression (10) but often this number can be substantially reduced due to the particularities of the considered systems.

Subtle adjustments of the exposed ideas and the expression (10) unable to fulfill with two other objectives; give approximations to periodic solutions whose amplitude goes beyond the limits of locality by the graphical Hopf method (Example 1 in the next section) and provide approximations for the second period doubling bifurcation and also for the corresponding limit cycles (Example 2).

5. Applications

Example 1. Consider the classic Rössler system [23]

$$\begin{aligned} \dot{x}_1 &= -x_2 - x_3, \\ \dot{x}_2 &= x_1 + ax_2, \\ \dot{x}_3 &= b + x_3(x_1 - c), \end{aligned} \quad (11)$$

where a, b, c are parameters and a unique nonlinearity is distinguished in the third equation. The general form of the equilibrium points of the given system is

$$\begin{aligned}\tilde{x}_1 &= \tilde{x}_1(a, b, c) = \frac{c}{2} \pm \frac{\sqrt{c^2 - 4ab}}{2}, \\ \tilde{x}_2 &= \tilde{x}_2(a, b, c) = -\frac{c}{2a} \mp \frac{\sqrt{c^2 - 4ab}}{2a}, \\ \tilde{x}_3 &= \tilde{x}_3(a, b, c) = \frac{c}{2a} \pm \frac{\sqrt{c^2 - 4ab}}{2a},\end{aligned}$$

but under certain conditions that are assumed below, the equilibrium results stable when $\tilde{x}_1 = \frac{c}{2} - \frac{\sqrt{c^2 - 4ab}}{2}$.

Observation: Precise formulae to analyze the stability of equilibrium points of (11) can be derived through Routh–Hurwitz criterium.

Defining the following matrices

$$A = \begin{bmatrix} 0 & -1 & -1 \\ 1 & a & 0 \\ 0 & 0 & -c \end{bmatrix}, \quad B = \begin{bmatrix} 0 \\ 0 \\ 1 \end{bmatrix}, \quad C = \begin{bmatrix} 1 & 0 & 0 \\ 0 & 0 & 1 \end{bmatrix}, \quad D = [0 \quad 0],$$

system (11) can be written as

$$\begin{aligned}\dot{x} &= Ax + BDy + B[\tilde{g}(y; (a, b, c)) - Dy], \\ y &= Cx,\end{aligned}$$

where $x = [x_1 \ x_2 \ x_3]^T$ and $y = [y_1 \ y_3]^T$, yielding a linear part G

$$G(s; (a, b, c)) = C(sI - A)^{-1}B = \frac{1}{\Delta_1(s)} \begin{bmatrix} -(s - a) \\ s(s - a) + 1 \end{bmatrix},$$

where $\Delta_1(s) = (s + c)(s^2 - as + 1)$ and a nonlinear part u

$$u = g(e; (a, b, c)) = (\tilde{g}(y; (a, b, c)) - Dy)|_{y=-e} = [b + e_1 e_3].$$

Solving the corresponding equation (3), one obtains

$$\tilde{e} = [\tilde{e}_1 \ \tilde{e}_3]^T = \left[-\frac{c}{2} + \frac{\sqrt{c^2 - 4ab}}{2} \quad \frac{\tilde{e}_1}{a} \right]^T,$$

and the matrix J defined in (4) results

$$J = D_1 g|_{e=\tilde{e}} = [\tilde{e}_3 \ \tilde{e}_1] = \left[\frac{\tilde{e}_1}{a} \quad \tilde{e}_1 \right].$$

It can be proved with the frequency domain formalism that a supercritical Hopf bifurcation occurs while varying the parameter c , for the parameter values $a = 0.5$, $b = 0.5944$, $c_0 = 1.146880195$ and frequency $\omega_0 = 1.189754010$. In this part of the example, it will be noted $\mu = c$ as the main or distinguished bifurcation parameter. Proposition 1 of Section 2 can be verified. In this sense, given that

$$h(-1, i\omega; \mu) = \det(-1 \times I - GJ) = F_1(\omega, \mu) + iF_2(\omega, \mu),$$

results

$$\begin{aligned}F_1(\omega, \mu) &= 1 + \frac{\tilde{e}_1[(2 - \omega^2) \operatorname{Re}(\Delta_1(i\omega)) - (a + a^{-1})\omega \operatorname{Im}(\Delta_1(i\omega))]}{\chi}, \\ F_2(\omega, \mu) &= \frac{-\tilde{e}_1[(2 - \omega^2) \operatorname{Im}(\Delta_1(i\omega)) + (a + a^{-1})\omega \operatorname{Re}(\Delta_1(i\omega))]}{\chi},\end{aligned}$$

where $\tilde{e}_1 = -\frac{\mu}{2} + \frac{\sqrt{\mu^2 - 4ab}}{2}$, $\Delta_1(i\omega) = (a - \mu)\omega^2 + \mu + i\omega(1 - \omega^2 - a\mu)$ and $\chi = \Delta_1(i\omega)\overline{\Delta_1(i\omega)}$. Thus, as $\mu = \mu_0 = \mu_H$ follows:

$$F_1(\omega_0, \mu_H) = 0.15 \times 10^{-8}, \quad F_2(\omega_0, \mu_H) = -0.2751153108 \times 10^{-9},$$

proving Proposition 1. To verify the graphical Hopf theorem, its three hypotheses must be checked. The characteristic eigenlocus $\hat{\lambda}$, exactly at Hopf bifurcation, is depicted in Fig. 2. Besides, one obtains

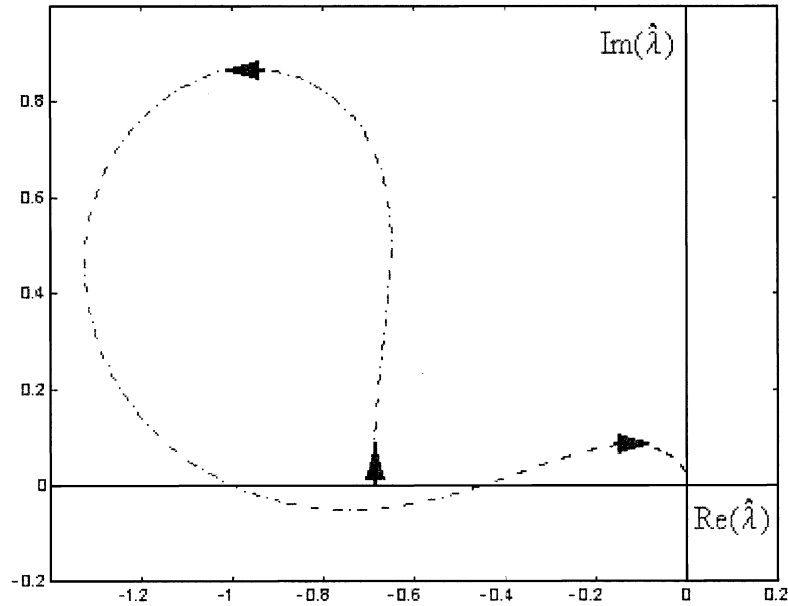


Fig. 2. Characteristic eigenlocus $\hat{\lambda}$ for Rössler system (11) at Hopf bifurcation ($a = 0.5, b = 0.5944, \mu_H = 1.146880195$).

$$M_1 = \left| \frac{\partial(F_1, F_2)}{\partial(\omega, \mu)} \Big|_{(\omega_0, \mu_H)} \right| = 2.084622624 \neq 0.$$

From the cumbersome computation of the curvature coefficient (6), it results

$$\sigma_1 = -0.04829905280 \neq 0.$$

According with the obtained outcomes, it can be asserted that a branch of stable periodic solutions arises at μ_H (super-critical Hopf bifurcation) and spreads to the right (based on the unfolding of $\hat{\lambda}$ as μ varies next to μ_H).

To attain the determination of the limit cycles approximation, one proceeds as it has been described in Section 2. The development of the proposed example is very laborious due to (11) does not result a SISO (single input–single output) system, with the suggested realization. The normalized vectors u and v ($|v| = 1$ and $\bar{u}^T v = 1$), that appear in the expression (6), have order 2×1 with complex components in contrast to SISO systems where u and v can be considered identically 1 and the vector $V_{13} = 0$. In the case of harmonic balance of order two, one must compute the vector V_{13} according with Eq. (8), and subsequently V_{15}, V_{17} and V_{19} for higher order balances [16,18].

Considering $\tilde{\mu} = 1.16$, when the solutions given by the different order balances are built up and its monodromy matrices are analyzed, one obtains the trivial multipliers that appear in Table 1. Although the trivial multiplier is alike under four, six and eight order balances (for short HB4, HB6, and HB8, respectively), the component x_2 becomes precise just when eight harmonics are involved in its approximate expression.

By way of example, when the tool is the harmonic balance of second order (HB2), the expressions of the components x_1 and x_3 result

$$x_{1(2)}(t; \tilde{\mu}) = 0.3968554773 + 0.1087821998 \cos(\hat{\omega}t) + 0.2586111072 \sin(\hat{\omega}t) - 0.5282411513 \times 10^{-2} \cos(2\hat{\omega}t) + 0.5416165840 \times 10^{-3} \sin(2\hat{\omega}t),$$

Table 1

Comparison of trivial multipliers according to different balance orders for a limit cycle in Rössler system with $a = 0.5, b = 0.5944, \tilde{\mu} = 1.16$

HB2	HB4	HB6	HB8
1.001172230	1.000615281	1.000605369	1.000605215

$$x_{3(2)}(t; \bar{\mu}) = 0.7937109546 - 0.9232660253 \times 10^{-1} \cos(\hat{\omega}t) + 0.1298139085 \sin(\hat{\omega}t) - 0.1516745424 \times 10^{-2} \times \cos(2\hat{\omega}t) - 0.1037931236 \times 10^{-1} \sin(2\hat{\omega}t),$$

where $\hat{\omega} = \hat{\omega}_{(2)} = 1.188260342$ and $\hat{\theta} = \hat{\theta}_{(2)} = 0.3226284489$. With these last formulae, the variable x_2 can be obtained from the first equation of system (11). A thorough application of the generalization of the graphical Hopf method allows to achieve the approximate expression of the cycle using eight harmonics (HB8) and its representation together with the numerical one obtained by using LOCBIF [12] can be observed in Fig. 3.

It is known that the graphical Hopf method has local validity and its accuracy depends on the amplitude of the studied cycle (the method is really precise if the amplitude θ is much less than 1). Moreover, the variational equation for Rössler system, (11), results

$$\dot{z} = D(t)z, \quad \text{where } D(t) = \begin{bmatrix} 0 & -1 & -1 \\ 1 & a & 0 \\ x_3(t; \mu) & 0 & x_1(t; \mu) - \mu \end{bmatrix},$$

and the comparison of the multipliers of the two analyzed approximations is shown in Table 2.

Now let us show when this procedure is deficient in obtaining a precise quasi-analytical expression, i.e., when a limit cycle \mathbf{X} has amplitude $\hat{\theta}$ which is close or larger than 1. It is reported that the system (11) undergoes a supercritical Hopf bifurcation for $a_0 = 0.124967501$, $b = 2$ and $c = 4$, and now a is considered as the main bifurcation parameter. Therefore, for the rest of the development of this example, is noted $\mu = a$. Particularly, if $\mu = 0.13$, $b = 2$, $c = 4$, there is a limit cycle with frequency $\hat{\omega} = \hat{\omega}_{(2)} = 1.008515860$ (chosen by the trivial multiplier exactness test) and amplitude $\hat{\theta} = \hat{\theta}_{(2)} = 0.9354726026$ (which is next to unity). It is supposed that the periodic solution has the following general form

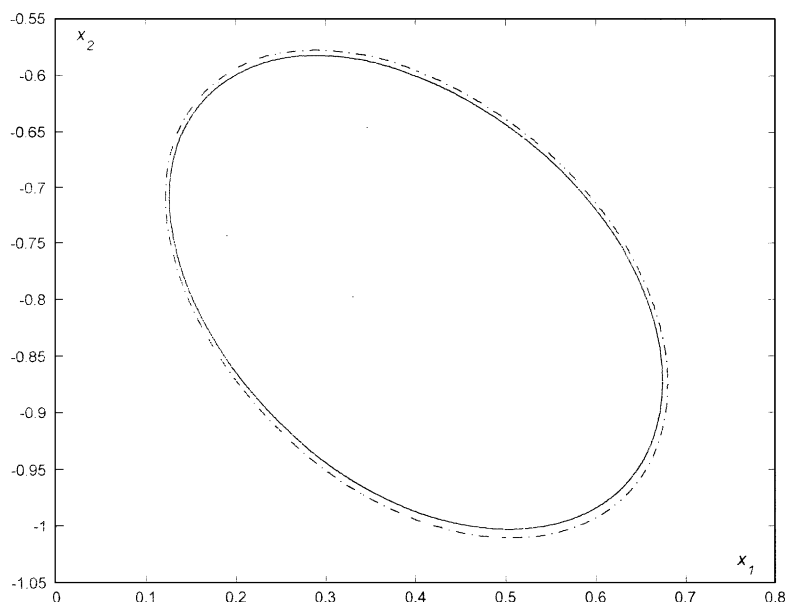


Fig. 3. Comparison of periodic solutions for Rössler system (11) with $a = 0.5$, $b = 0.5944$, $\bar{\mu} = 1.16$ (small amplitude cycle): LOCBIF (---) and HB8 (—).

Table 2

Comparison of Floquet multipliers for a limit cycle in Rössler system with $a = 0.5$, $b = 0.5944$, $\bar{\mu} = 1.16$ (small amplitude cycle)

	LOCBIF	HB8
α_0	0.9999996	1.000605215
α_1	0.9498978	0.9469734053
α_2	0.2613515	0.2622177935

$$\mathbf{X}(t; \tilde{\mu}) = (x_i(t; \tilde{\mu})) = \sum_{j=0}^2 a_{i,j} \cos(j\hat{\omega}t) + \sum_{k=1}^2 b_{i,k} \sin(k\hat{\omega}t),$$

where $\hat{\omega} = \hat{\omega}_{(2)}$ is the most precise approximate frequency of the limit cycle, and $a_{i,j}$, $b_{i,k}$, $i = 1, \dots, n$, are numerical vectors to compute. Starting from an expression for the component x_2 such as

$$x_2(t; 0.13) = a_{2,0} + a_{2,1} \cos(\hat{\omega}t) + a_{2,2} \cos(2\hat{\omega}t) + b_{2,1} \sin(\hat{\omega}t) + b_{2,2} \sin(2\hat{\omega}t),$$

introducing it in system (11) and executing an elementary harmonic balance of second order in $\hat{\omega}$, with an initial vector $Z = [-0.55 \ 0.95 \ 0.1 \ 0.1 \ 0.1]$, results

$$x_2(t; 0.13) = -0.52240495570849 + 0.90896152983970 \cos(\hat{\omega}t) - 0.333981492076 \times 10^{-2} \cos(2\hat{\omega}t) \\ + 0.8210187782669 \times 10^{-1} \sin(\hat{\omega}t) - 0.264690187575 \times 10^{-2} \sin(2\hat{\omega}t),$$

from where the expressions of x_1 and x_3 can be obtained using the second and the first equation of the system (11), respectively.

Otherwise, the approximations of the component x_2 , resulting from second and fourth order balances by the graphical Hopf method are:

$$x_{2(2)}(t; 0.13) = -0.5222403102 + 0.8567493460 \cos(\hat{\omega}_{(2)}t) - 0.2385459863 \times 10^{-2} \cos(2\hat{\omega}_{(2)}t) + 0.1061395514 \\ \times \sin(\hat{\omega}_{(2)}t) - 0.4311948699 \times 10^{-2} \sin(2\hat{\omega}_{(2)}t),$$

and

$$x_{2(4)}(t; 0.13) = -0.5223012501 + 0.8618262509 \cos(\hat{\omega}_{(4)}t) - 0.3222695438 \times 10^{-2} \cos(2\hat{\omega}_{(4)}t) - 0.1799462176 \\ \times 10^{-3} \cos(3\hat{\omega}_{(4)}t) - 0.2013544557 \times 10^{-5} \cos(4\hat{\omega}_{(4)}t) + 0.1941740708 \times 10^{-1} \sin(\hat{\omega}_{(4)}t) \\ - 0.3772189876 \times 10^{-2} \sin(2\hat{\omega}_{(4)}t) - 0.5631903787 \times 10^{-4} \sin(3\hat{\omega}_{(4)}t) + 0.8945067199 \times 10^{-5} \\ \times \sin(4\hat{\omega}_{(4)}t),$$

respectively, where $\hat{\omega}_{(4)} = 1.008524147$.

The representation of the solution achieved with the graphical Hopf theorem which results most precise (HB2 in this case) has been compared with the proposed approximation and also with the numerical one obtained with LOCBIF [12] and they are shown in Fig. 4. It is remarkable the coincidence between the outcomes of LOCBIF and the described

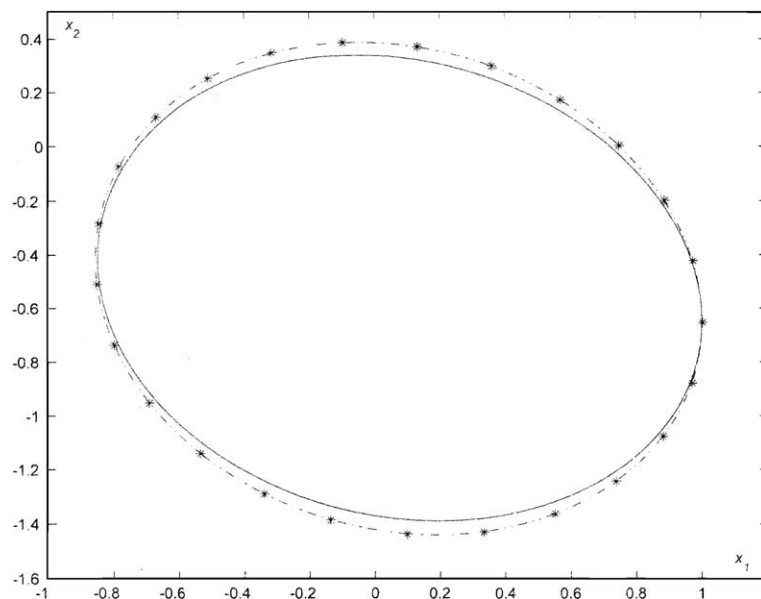


Fig. 4. Comparison of periodic solutions for Rössler system (11) with $\tilde{\mu} = 0.13$, $b = 2$, $c = 4$ (medium amplitude cycle): LOCBIF (*), HB2 (—), and proposed approximation (---).

Table 3

Comparison of Floquet multipliers for a limit cycle in Rössler system with $\tilde{\mu} = 0.13, b = 2, c = 4$ (medium amplitude cycle)

	LOCBIF	HB2	Proposed approximation
α_0	1.000000	1.001855109	0.9999686861
α_1	$-0.8879129 \times 10^{-5}$	$0.5402100989 \times 10^{-10}$	$0.3097166967 \times 10^{-10}$
α_2	0.9688779	0.9691623943	0.9688645116

procedure. Moreover, the multipliers associated to the three approximations appear in Table 3, where the agreement, is visible through the results depicted in Fig. 4.

Carrying on the analysis for large amplitude cycles ($\hat{\theta}$ larger than 1), it is considered $\tilde{\mu} = 0.15, b = 2, c = 4$, where the most precise amplitude and frequency values of the Hopf cycle result: $\hat{\theta} = \hat{\theta}_{(2)} = 1.936235807 \approx 2$ and $\hat{\omega} = \hat{\omega}_{(2)} = 1.010496960$ after using a second order harmonic balance. Replaying the earlier proposal, starting now with the initial vector $Z = [-0.55 \ 1.95 \ 0.1 \ 0.1 \ 0.1]$, it is obtained the following expression:

$$x_2(t; 0.15) = -0.57841872820727 + 1.87215612990062 \cos(\hat{\omega}t) - 0.1771864802786 \times 10^{-1} \cos(2\hat{\omega}t) + 0.6907228540357 \times 10^{-1} \sin(\hat{\omega}t) - 0.1119340859546 \times 10^{-1} \sin(2\hat{\omega}t).$$

Newly, the coincidence of results coming from LOCBIF [12] and those achieved with the proposed methodology is noticeable, as can be seen in Fig. 5. Now, in Table 4 the characteristic multipliers are analyzed, where those coming from the approximations obtained with the graphical Hopf method have been neglected due to the large error in the trivial multiplier. Considering the multiplier α_0 , it can be asserted that the proposed approximation has lost some

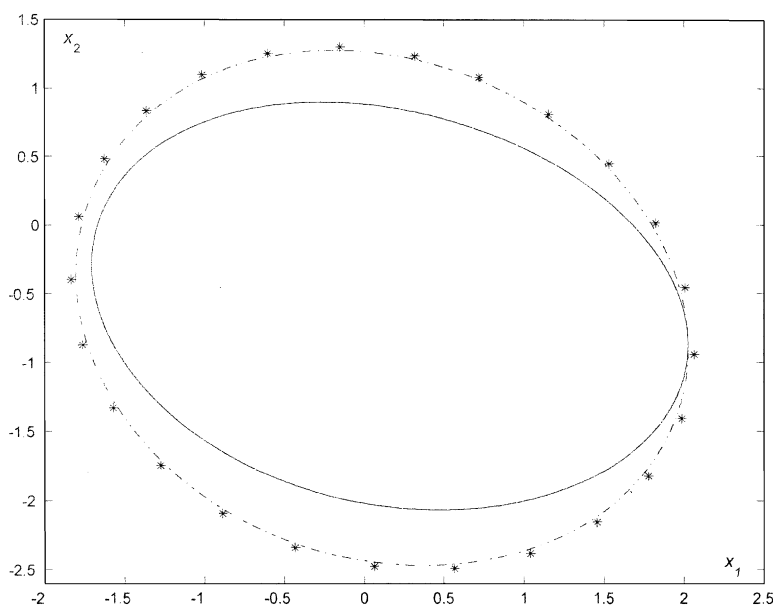


Fig. 5. Comparison of periodic solutions for Rössler system (11) with $\tilde{\mu} = 0.15, b = 2, c = 4$ (large amplitude cycle): LOCBIF (*), HB2 (—), and proposed approximation (- · -).

Table 4

Comparison of Floquet multipliers for a limit cycle in Rössler system with $\tilde{\mu} = 0.15, b = 2, c = 4$ (large amplitude cycle)

	LOCBIF	Proposed approximation
α_0	1.000000	0.9998882927
α_1	0.3450×10^{-6}	$0.6872591421 \times 10^{-10}$
α_2	0.8306614	0.8313191601

precision, regarding the case with $\tilde{\mu} = 0.13$. Despite of this reflection, the obtained results amply exceed those given by the graphical Hopf method. The use of the monodromy matrix allows to predict a validity interval for the approximations of the oscillations, starting at Hopf bifurcation as far as the trivial multiplier remains in a certain and acceptable neighborhood of the value 1. Henceforth, other quasi-analytical techniques should be used to recover the solutions properly.

Example 2. The following system has been analyzed by Tesi et al. [27] regarding the delay of the period doubling cascade by means of feedback control

$$\begin{aligned}\dot{x}_1 &= x_2, \\ \dot{x}_2 &= x_3, \\ \dot{x}_3 &= -x_1 - 1.2x_2 + \mu x_3 + x_1^2,\end{aligned}\tag{12}$$

where $\mu \in \mathbb{R}$ is the bifurcation parameter of the given system. There are two equilibrium points, say, $\tilde{x}_{1,1} = 0$, $\tilde{x}_{1,2} = 1$, $\tilde{x}_2 = \tilde{x}_3 = 0$ yet it is known that only with $\tilde{x}_{1,1} = 0$ a supercritical Hopf bifurcation arises when $\mu_H = -\frac{5}{6} \approx -0.833$ and its critical frequency results $\omega_0 = \sqrt{-\mu_H^{-1}} \approx 1.095445115$.

If the realization is considered with

$$A = \begin{bmatrix} 0 & 1 & 0 \\ 0 & 0 & 1 \\ -1 & -1.2 & \mu \end{bmatrix}, \quad B = \begin{bmatrix} 0 \\ 0 \\ 1 \end{bmatrix}, \quad C = [1 \quad 0 \quad 0], \quad D = -1,$$

the system (12) becomes

$$\begin{aligned}\dot{x} &= Ax + BDy + B[\tilde{g}(y; \mu) - Dy], \\ y &= Cx, \\ u &= g(e; \mu),\end{aligned}$$

where $\tilde{g}(y; \mu) = y_1^2$, $g(e; \mu) = (\tilde{g}(y; \mu) - Dy)|_{y=-e} = (y_1^2 + y_1)|_{y_1=-e_1} = e_1^2 - e_1$. Thereby, the transfer function $G(s; \mu)$ results

$$G(s; \mu) = C(sI - A)^{-1}B = \frac{1}{\Delta_2(s)},$$

where $\Delta_2(s) = s^3 - \mu s^2 + 1.2s + 2$.

According with (3), the frequency domain equilibrium points are: $\tilde{e}_{1,1} = 0$ and $\tilde{e}_{1,2} = -1$ but only the first is related to Hopf bifurcation. Moreover, with the suggested realization, the matrix J is

$$J = D_1 g|_{e_1=\tilde{e}_{1,1}} = 2\tilde{e}_{1,1} - 1 = -1.$$

To show the implementation of the graphical Hopf method, it is considered the value $\tilde{\mu} = -0.8 > \mu_H$, with the goal of obtaining the quasi-analytical approximation of the limit cycle. Using harmonic balance of eighth order, the following expression for the component x_1 follows:

$$\begin{aligned}x_{1(8)}(t; \tilde{\mu}) &= 0.02128105998 - 0.2040839981 \cos(\hat{\omega}_{(8)}t) - 0.8543361336 \times 10^{-3} \cos(2\hat{\omega}_{(8)}t) - 0.2336150921 \\ &\quad \times 10^{-2} \sin(2\hat{\omega}_{(8)}t) + 0.1303079731 \times 10^{-4} \cos(3\hat{\omega}_{(8)}t) - 0.8718147851 \times 10^{-5} \sin(3\hat{\omega}_{(8)}t) \\ &\quad + 0.5774010851 \times 10^{-7} \cos(4\hat{\omega}_{(8)}t) + 0.5331336598 \times 10^{-7} \sin(4\hat{\omega}_{(8)}t) - 0.1715095199 \times 10^{-9} \\ &\quad \times \cos(5\hat{\omega}_{(8)}t) + 0.3002211224 \times 10^{-9} \sin(5\hat{\omega}_{(8)}t) - 0.1340401168 \times 10^{-11} \cos(6\hat{\omega}_{(8)}t) \\ &\quad - 0.4076862615 \times 10^{-12} \sin(6\hat{\omega}_{(8)}t) + 0.4699758907 \times 10^{-15} \cos(7\hat{\omega}_{(8)}t) - 0.5372921492 \times 10^{-14} \\ &\quad \times \sin(7\hat{\omega}_{(8)}t) + 0.1966077060 \times 10^{-16} \cos(8\hat{\omega}_{(8)}t) - 0.2604125289 \times 10^{-17} \sin(8\hat{\omega}_{(8)}t),\end{aligned}$$

where $\hat{\omega}_{(8)} = 1.094470341$ and returning to (12), the expressions for the variables x_2 and x_3 can be attained easily. In this specific case, it is interesting to perceive the improvement in the results achieved by different order harmonic balances, watching the error of the trivial multiplier estimation (compare it with equivalent results in [5] for sixth order harmonic balance). This is presented in Table 5.

A continuation of the periodic solution branch can be worked out until the detection of the first period doubling bifurcation that is found at $\mu_{PD2} = -0.4847$ where the cycle amplitude results $x_{1\max} = 0.799$. This can be checked through Table 6. Furthermore, these results have been verified with LOCBIF which detects the first period doubling

Table 5

Comparison of trivial multipliers according to different balance orders for Tesi system with $\tilde{\mu} = -0.8$

HB2	HB4	HB6	HB8
1.000058159	0.9999882234	1.000000389	1.000000033

Table 6

Flip or period doubling bifurcation detection for Tesi system through graphical Hopf method of order 8 (HB8)

	$\mu = -0.4847$	$\mu = -0.4846$
α_0	1.000090421	1.000090532
α_1	-0.9999329740	-1.000889654
α_2	-0.6061405358	-0.6059079536

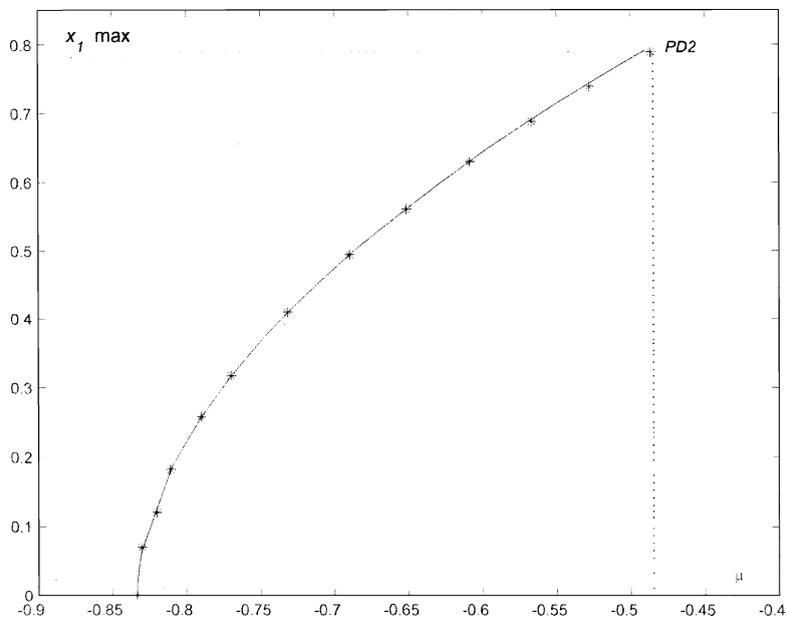


Fig. 6. Continuation of periodic solutions branch for Tesi system (12): (*) LOCBIF and (—) estimation by the graphical Hopf method (HB8).

bifurcation for $\mu_{PD2}^* = -0.480927$. Both periodic branches are depicted in Fig. 6. The occurrence of this bifurcation makes that the Hopf cycle changes its stability, turning from stable to unstable and originates a new stable solution whose period duplicates the one of the former cycle. A supercritical period doubling bifurcation is defined wholly by these events. In the remaining of this section it is attempted to give quasi-analytical approximations of these new sub-harmonic solutions.

According to the particularities of system (12) and the formula (10), it is proposed the following expression for the first component of the period doubling orbit

$$x_{1(PD2)}(t; \tilde{\mu}) = \sum_{j=0}^4 a_{1,j} \cos\left(j \frac{\hat{\omega}}{2} t\right) + \sum_{k=1}^4 b_{1,k} \sin\left(k \frac{\hat{\omega}}{2} t\right), \tag{13}$$

where $a_{1,j}, b_{1,k}$ are numerical constants to find, and $\hat{\omega}$ is the frequency of the Hopf cycle that coexists with the first period doubling solution for a certain value of $\tilde{\mu}$ larger than μ_{PD2} , chosen in agreement with Section 4. Taking this expression to system (12), operating in the three equations and executing a fourth order balance with frequency $\frac{\hat{\omega}}{2}$, it is achieved a nonlinear algebraic system, whose solution enables to write the quasi-analytical expression of the period

doubling orbit. To illustrate the methodology, three different cases have been analyzed whereas the parameter $\tilde{\mu}$ moves away from the bifurcation value μ_{PD2} , namely, $\mu_I = -0.48$, $\mu_{II} = -0.4633$ and $\mu_{III} = -0.435$. In the three considered situations, the starting value $\hat{\omega}$ arises from applying the eighth order balance, say, $\hat{\omega} = \hat{\omega}_{(8)}$.

Beginning with $\mu_I = -0.48$, one finds a limit cycle with frequency $\hat{\omega}_{(8)} = 1.086316552$ and first component amplitude $\hat{\theta}_{(8)} = 0.58929$, reaching $x_{1max} = 0.80489$. With the method described above and the initial vector $Z = [0 \ 0.025 \ 0.6 \ 0.1 \ 0.1 \ 0.1 \ 0.1 \ 0.1 \ 0.1]$, the following approximate expression for the component $x_{1(PD2)}$ has been obtained

$$\begin{aligned} x_{1(PD2)}(t; \mu_I) = & 0.21889767624362 + 0.2513089233007 \times 10^{-1} \cos\left(\frac{1}{2}\hat{\omega}t\right) + 0.54457984910603 \cos(\hat{\omega}t) \\ & + 0.355813539338 \times 10^{-2} \cos\left(\frac{3}{2}\hat{\omega}t\right) + 0.1071714999275 \times 10^{-1} \cos(2\hat{\omega}t) + 0.14296567650609 \\ & \times 10^{-1} \sin\left(\frac{1}{2}\hat{\omega}t\right) + 0.20982731737460 \sin(\hat{\omega}t) - 0.559190530143 \times 10^{-2} \sin\left(\frac{3}{2}\hat{\omega}t\right) \\ & - 0.1891960621980 \times 10^{-1} \sin(2\hat{\omega}t). \end{aligned}$$

Taking this result to system (12), the whole quasi-analytical expression of the bifurcated orbit is attained. The comparison between the proposed approximation and the numerical one which comes from LOCBIF is shown in Fig. 7. On the other hand, evaluating the characteristic multipliers of the corresponding monodromy matrix D_I , namely

$$D_I(t) = \begin{bmatrix} 0 & 1 & 0 \\ 0 & 0 & 1 \\ -1 + 2x_{1(PD2)}(t; \mu_I) & -1.2 & \mu_I \end{bmatrix},$$

one obtains the results that are exhibited in Table 7. Therefore, the similarity of the multipliers allows to assert that the approximation is really good. Furthermore, the new subharmonic solution is stable in agreement with the results of

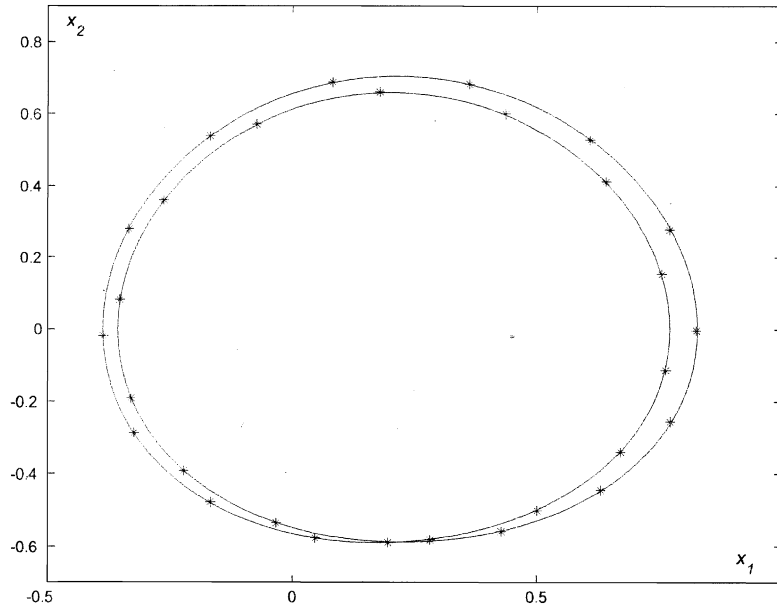


Fig. 7. Comparison of period doubling solutions for Tesi system (12) with $\mu_I = -0.48$: (*) LOCBIF and (—) proposed approximation.

Table 7
Comparison of characteristic multipliers for Tesi system with $\mu_I = -0.48$

	LOCBIF	Proposed approximation
$\alpha_0(PD2)$	0.9999994	1.001896861
$\alpha_1(PD2)$	0.9646491	0.9598248056
$\alpha_2(PD2)$	0.40244×10^{-2}	$0.4032095854 \times 10^{-2}$

Section 3 due to $|\alpha_{i(\text{PD2})}| < 1, i = 1, 2$, and has right precision (see $\alpha_{0(\text{PD2})}$). Moreover, it must be noted that the period of the proposed solution is $T = 11.568$ which results almost equal to LOCBIF's: $T_{\text{LOCBIF}} = 11.563$.

Regarding the parameter value $\mu_{\text{II}} = -0.4633$, the Hopf cycle has frequency $\hat{\omega}_{(8)} = 1.085950159$ and $\hat{\theta}_{(8)} = 0.59949$ as the amplitude for its first component. With this information and considering the vector $Z = [0 \ 0.1 \ 0.59 \ 0.1 \ 0.1 \ 0.1 \ 0.1 \ 0.1 \ 0.1]$, the nonlinear system determined by (13) is solved and then follows:

$$\begin{aligned} x_{1(\text{PD2})}(t; \mu_{\text{II}}) = & 0.22518179491674 + 0.10098107964686 \cos\left(\frac{1}{2}\hat{\omega}t\right) + 0.51687041752347 \cos(\hat{\omega}t) \\ & + 0.1821723338030 \times 10^{-1} \cos\left(\frac{3}{2}\hat{\omega}t\right) + 0.1381822888703 \times 10^{-1} \cos(2\hat{\omega}t) \\ & + 0.6466091529452 \times 10^{-1} \sin\left(\frac{1}{2}\hat{\omega}t\right) + 0.25789176476450 \sin(\hat{\omega}t) - 0.2041177655416 \times 10^{-1} \sin\left(\frac{3}{2}\hat{\omega}t\right) \\ & - 0.1651329316608 \times 10^{-1} \sin(2\hat{\omega}t). \end{aligned}$$

The eigenvalues of the monodromy matrix D_{II} result $\alpha_{0(\text{PD2})} = 0.9997533768, \alpha_{1(\text{PD2})} = 0.2784811278, \alpha_{2(\text{PD2})} = 0.1686438027 \times 10^{-1}$. Furthermore, as the characteristic multipliers of the numerical solution are $\alpha_{0(\text{LOCBIF})} = 0.9999997, \alpha_{1(\text{LOCBIF})} = 0.3165313, \alpha_{2(\text{LOCBIF})} = 0.149580 \times 10^{-1}$ it is observed that exists a rather evident discrepancy with the value of α_1 . In spite of the last observation, the coincidence of results between the quasi-analytical solution and LOCBIF's is remarkable, as can be seen in Fig. 8.

The explained methodology enables to achieve very accurate approximations even in the vicinity of the next or second period doubling bifurcation, noted as PD4. Just to give an example, it is selected the value $\mu_{\text{III}} = -0.435$, where $\hat{\omega}_{(8)} = 1.085341359$ and $\hat{\theta}_{(8)} = 0.61585$. Using the vector $Z = [0 \ 0.35 \ 0.53 \ 0.1 \ 0.1 \ 0.1 \ 0.1 \ 0.1 \ 0.1]$ as starting point, one obtains the proposed solution and its characteristic multipliers result $\alpha_{0(\text{PD2})} = 0.9961836760, \alpha_{1(\text{PD2})} = -0.7981672154, \alpha_{2(\text{PD2})} = -0.8170013202 \times 10^{-2}$, while those belonging to the numerical one are $\alpha_{0(\text{LOCBIF})} = 0.9999996, \alpha_{1(\text{LOCBIF})} = -0.8511485, \alpha_{2(\text{LOCBIF})} = -0.77888 \times 10^{-2}$. Both solutions are contrasted in Fig. 9 and it must be noted that the difference between the corresponding periods is stressed now, having $T = 11.578$ versus $T_{\text{LOCBIF}} = 11.532$ (though this fact is not reflected in the figure just observed).

With the information given above, it can be asserted that as the parameter μ moves away from Hopf bifurcation, it is deepened the difference of the Floquet multipliers of the proposed solution versus LOCBIF ones, and this yields a significant distortion when one intends to find the value of μ where the second period doubling bifurcation takes place, symbolized as $\mu_2 \triangleq \mu_{\text{PD4}}$. According with LOCBIF, this bifurcation results at $\mu_{\text{PD4}}^* = -0.431768$, whereas with the suggested technique one achieves $\mu_{\text{PD4}} = -0.428$. Thus, the period-2 cycle becomes unstable and coexists with a new

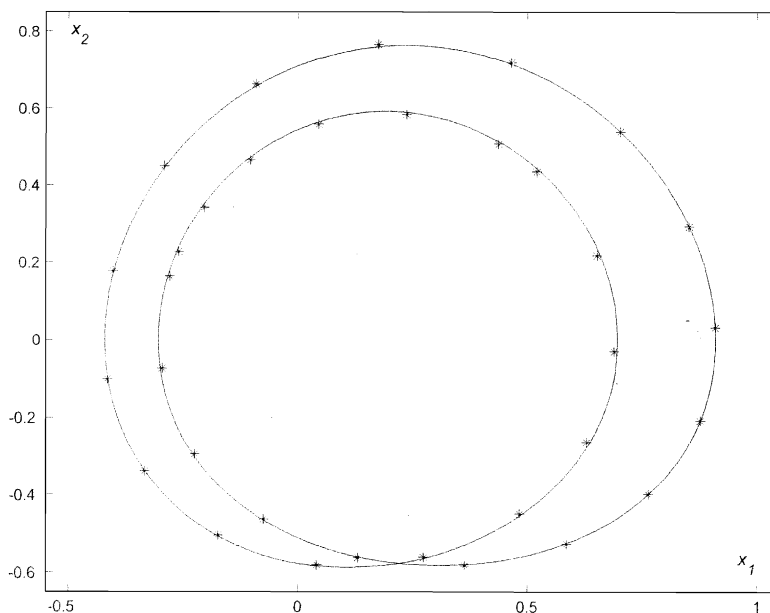


Fig. 8. Comparison of period doubling solutions for Tesi system (12) with $\mu_{\text{II}} = -0.4633$: (*) LOCBIF and (—) proposed approximation.

period-4 orbit which is stable. Particularly, it is examined when $\mu_{IV} = -0.426$, where the leading information is $\hat{\omega}_{(8)} = 1.085150860$ and $\hat{\theta}_{(8)} = 0.6208346759$, proposing the following pattern:

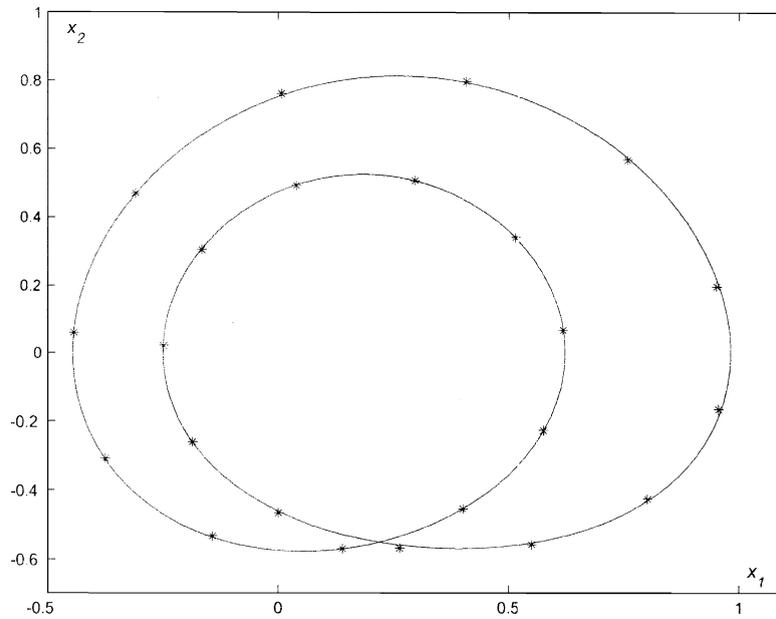


Fig. 9. Comparison of period doubling solutions for Tesi system (12) with $\mu_{III} = -0.435$: (*) LOCBIF and (—) proposed approximation.

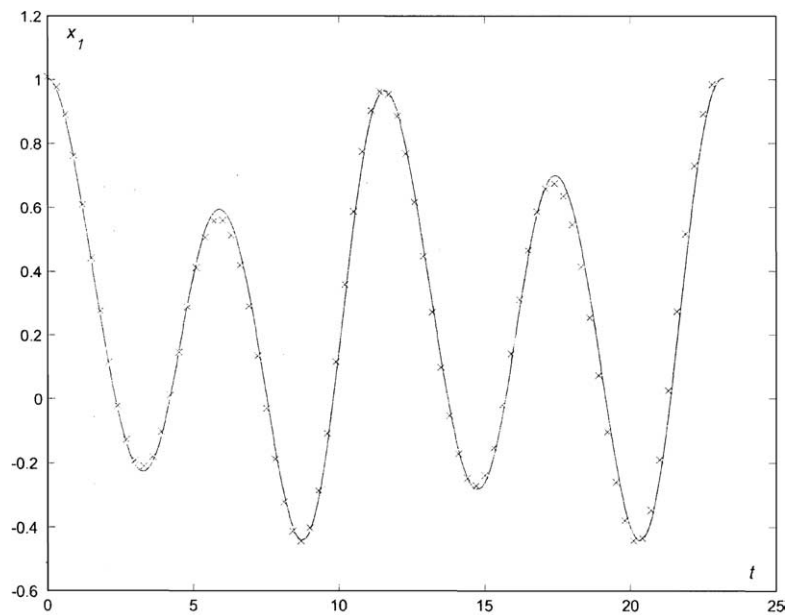


Fig. 10. Component x_1 for second period doubling solutions for Tesi system (12) with $\mu_{IV} = -0.426$: (x) LOCBIF and (—) proposed approximation.

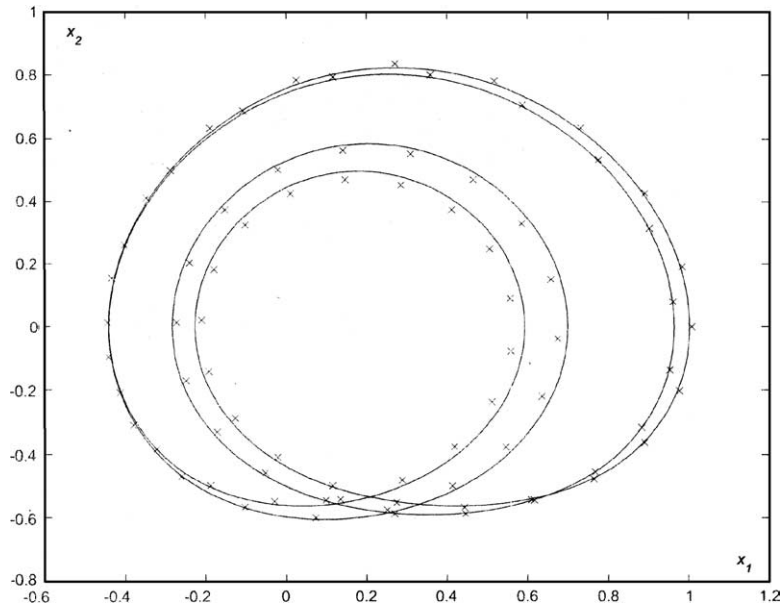


Fig. 11. Comparison of second period doubling solutions for Tesi system (12) with $\mu_{IV} = -0.426$: (x) LOCBIF and (—) proposed approximation.

$$x_{1(\text{PD4})}(t; \mu_{IV}) = \sum_{j=0}^8 c_{1,j} \cos\left(j \frac{\hat{\omega}}{4} t\right) + \sum_{k=1}^8 d_{1,k} \sin\left(k \frac{\hat{\omega}}{4} t\right),$$

where $c_{1,j}$ and $d_{1,k}$ are numerical constants to find. Fitting the period doubling argument with the initial vector $Z = [z_{1,i}]$, $i = 1, \dots, 17$ where $z_{1,1} = 0.24$, $z_{1,2} = z_{1,4} = z_{1,10} = z_{1,12} = 0.01$, $z_{1,3} = z_{1,6} = z_{1,7} = z_{1,8} = z_{1,9} = z_{1,11} = z_{1,14} = z_{1,15} = z_{1,16} = z_{1,17} = 0.1$, $z_{1,5} = 0.3$, $z_{1,13} = 0.48$, one states:

$$\begin{aligned} x_{1(\text{PD4})}(t; \mu_{IV}) = & 0.24201810098281 + 0.2348739060806 \times 10^{-1} \cos\left(\frac{1}{4}\hat{\omega}t\right) + 0.10711848604380 \cos\left(\frac{1}{2}\hat{\omega}t\right) \\ & - 0.1847585036934 \times 10^{-1} \cos\left(\frac{3}{4}\hat{\omega}t\right) + 0.25501496965284 \cos(\hat{\omega}t) \\ & + 0.836805908637 \times 10^{-2} \cos\left(\frac{5}{4}\hat{\omega}t\right) + 0.3913593217349 \times 10^{-1} \cos\left(\frac{3}{2}\hat{\omega}t\right) \\ & + 0.3224027208 \times 10^{-4} \cos\left(\frac{7}{4}\hat{\omega}t\right) + 0.1991940006355 \times 10^{-1} \cos(2\hat{\omega}t) \\ & - 0.998792868734 \times 10^{-2} \sin\left(\frac{1}{4}\hat{\omega}t\right) + 0.13716011436851 \sin\left(\frac{1}{2}\hat{\omega}t\right) \\ & + 0.2469257746354 \times 10^{-1} \sin\left(\frac{3}{4}\hat{\omega}t\right) + 0.51639332738788 \sin(\hat{\omega}t) \\ & - 0.998219974513 \times 10^{-2} \sin\left(\frac{5}{4}\hat{\omega}t\right) + 0.673288704952 \times 10^{-2} \sin\left(\frac{3}{2}\hat{\omega}t\right) \\ & + 0.304615406774 \times 10^{-2} \sin\left(\frac{7}{4}\hat{\omega}t\right) + 0.892578653946 \times 10^{-2} \sin(2\hat{\omega}t), \end{aligned}$$

and its graphical representation is shown in Fig. 10, where the results obtained with LOCBIF are also included. It must be stand out the large complexity of considering this determination through the proposed methodology. In spite of this observation, the stability test has been performed again using the monodromy matrix and the characteristic multipliers have resulted $\alpha_{0(\text{PD4})} = 1.001014179$, $\alpha_{1(\text{PD4})} = -0.8919932945$, $\alpha_{2(\text{PD4})} = -0.5811276302 \times 10^{-4}$ whereas $\alpha_{0(\text{LOCBIF})} = 1.000000$, $\alpha_{1(\text{LOCBIF})} = -0.9190216 \times 10^{-1}$, $\alpha_{2(\text{LOCBIF})} = -0.5838424 \times 10^{-3}$. Therefore, the new approximation is quite precise and supports the stability of the period-4 orbit. As in the cases of the period-2 orbits examined before, the projection of both solutions in the phase plane (x_1, x_2) appears in Fig. 11.

6. Conclusions

In this paper, quasi-analytical approximations for period doubling oscillations close to Hopf bifurcations have been obtained. The methodology uses higher order harmonic balance to compute an accurate prediction of the periodic

branch from Hopf bifurcation until the departure of the trivial Floquet multiplier from +1 is noticeable. This fact marks the limit of the approximation of the oscillations using local methods. As the error of the approximation is acceptable, this technique seems to be powerful in order to analyze the unfoldings of certain codimension-two bifurcations involving one or more Hopf bifurcation curves in the space of system parameters. Such degeneracies are the double Hopf bifurcations [10] or the Gavrilov–Guckenheimer singularity [22], to mention only a few. It has been shown that in certain n -dimensional systems the period doubling bifurcation occurs when the parameterized amplitude θ is smaller than 1, and then the accuracy of the detected bifurcation is high. In these cases, a standard harmonic balance technique using $9n$ unknown coefficients is proposed to capture the subharmonic oscillations. In other cases, however, the amplitude of the parameterized amplitude θ surpasses the value 1 and then it is not possible to detect secondary bifurcations using local methods and even to continue the periodic branch. To remedy this situation, the same standard harmonic balance procedure is used and the initial conditions are fed with the data provided by the graphical Hopf method. This procedure can be adapted for the continuation of the periodic branch of high amplitude, as in Example 1, as well as for recovering the period doubling bifurcation, as shown in the Example 2.

Acknowledgments

G.R.I. acknowledges the support by Universidad Nacional del Comahue. J.L.M. appreciates the support of CONICET, Universidad Nacional del Sur and ANPCyT (PICT-11-12524). Both authors are thankful to the comments and help provided by Professor Hernán Cendra in several stages of the writing of this paper.

References

- [1] Allwright DJ. Harmonic balance and the Hopf bifurcation theorem. *Math Proc Cambridge Philos Soc* 1977;82:453–67.
- [2] Belhaq M, Houssni M. Symmetry-breaking and first period-doubling following a Hopf bifurcation in a three dimensional system. *Mech Res Commun* 1995;22(3):221–31.
- [3] Belhaq M, Freire E, Houssni M, Rodriguez-Luis AJ. Second period-doubling in a three dimensional system. *Mech Res Commun* 1999;26(2):123–8.
- [4] Ben-Tal A, Kirk V, Wake G. Banded chaos in power systems. *IEEE Trans Power Delivery* 2001;16(1):105–10.
- [5] Berns DW, Moiola JL, Chen G. Detecting period-doubling bifurcation: an approximate monodromy matrix approach. *Automatica* 2001;37:1787–95.
- [6] Bonani F, Gilli M. Analysis of stability and bifurcations of limit cycles in Chua's circuit through the harmonic-balance approach. *IEEE Trans Circ Syst I: Fundam Theory Appl* 1999;46(8):881–90.
- [7] Chen JH, Chau KT, Chan CC, Jiang Q. Subharmonics and chaos in switched reluctance motor drives. *IEEE Trans Energy Convers* 2002;17(1):73–8.
- [8] Chung KW, Chan CL, Xu J. An efficient method for switching branches of period-doubling bifurcations of strongly non-linear autonomous oscillators with many degrees of freedom. *J Sound Vib* 2003;267:787–808.
- [9] Hale J, Koçak H. Dynamics and bifurcations. New York: Springer-Verlag; 1991.
- [10] Itoich GR, Moiola JL. Double Hopf bifurcation analysis using frequency domain methods. *Nonlinear Dynam* 2005;39:235–58.
- [11] Jordan D, Smith P. Nonlinear differential equations. Avon, Great Britain: Oxford University Press; 1999.
- [12] Khibnik AI, Kuznetsov YA, Levitin VV, Nikolaev EV. Continuation techniques and interactive software for bifurcation analysis of ODE's and iterated maps. *Physica D* 1993;62:360–71.
- [13] Kuznetsov YA. Elements of applied bifurcation theory. New York: Springer-Verlag; 1995.
- [14] MacFarlane AG, Postlethwaite I. The generalized Nyquist stability criterion and multivariable root loci. *Int J Control* 1977;25:81–127.
- [15] Maggio GM, De Feo O, Kennedy MP. Nonlinear analysis of the Colpitts oscillator and applications to design. *IEEE Trans Circ Syst I: Fundam Theory Appl* 1999;46(9):1118–30.
- [16] Mees AI. Dynamics of feedback systems. Chichester, UK: John Wiley & Sons; 1981.
- [17] Mees AI, Chua L. The Hopf bifurcation theorem and its applications to nonlinear oscillations in circuits and systems. *IEEE Trans Circ Syst* 1979;6(4):235–54.
- [18] Moiola JL, Chen G. Hopf bifurcation analysis—A frequency domain approach. Singapore: World Scientific Publishing Co.; 1996.
- [19] Nayfeh A, Balachandran B. Applied nonlinear dynamics. New York: John Wiley & Sons; 1995.
- [20] Perez Velázquez J, Cortez M, Carter Snead III O, Wennberg R. Dynamical regimes underlying epileptiform events: role of instabilities and bifurcation in brain activity. *Physica D* 2003;16:205–20.
- [21] Rand RH. Analytical approximation for period-doubling following a Hopf bifurcation. *Mech Res Commun* 1989;16(2):117–23.
- [22] Robbio FI, Alonso DM, Moiola JL. Detection of limit cycle bifurcations using harmonic balance methods. *Int J Bifurcat Chaos* 2004;14(10):3647–54.
- [23] Rössler O. An equation for continuous chaos. *Phys Lett A* 1976;57(5):397–8.

- [24] Seydel R. Practical bifurcation and stability analysis. New York: Springer-Verlag; 1994.
- [25] Strumillo P, Ruta J. Poincaré mapping for detecting abnormal dynamics of cardiac repolarization. *IEEE Eng Med Bio Mag* 2002;21(1):62–5.
- [26] Tan C, Varghese M, Varaiya P, Wu F. Bifurcation, chaos and voltage collapse in power systems. *Proc IEEE* 1995;83(11):1484–96.
- [27] Tesi A, Abed EH, Genesio R, Wang HO. Harmonic balance analysis of period-doubling bifurcations with implications for control of nonlinear dynamics. *Automatica* 1996;2:1255–71.
- [28] Thompson JMT, Stewart HB. Nonlinear dynamics and chaos. Chichester, UK: John Wiley & Sons; 1986.
- [29] Torrini G, Genesio R, Tesi A. On the computation of characteristic multipliers for predicting limit cycle bifurcations. *Chaos, Solitons & Fractals* 1998;9(1/2):121–33.